analytical chemistry

Article

pubs.acs.org/ac

Analysis of a Common Cold Virus and Its Subviral Particles by Gas-Phase Electrophoretic Mobility Molecular Analysis and Native Mass Spectrometry

Victor U. Weiss,[†] Jessica Z. Bereszczak,[‡] Marlene Havlik,[†] Peter Kallinger,[§] Irene Gösler,[∥] Mohit Kumar,[∥] Dieter Blaas,[∥] Martina Marchetti-Deschmann,[†] Albert J. R. Heck,[‡] Wladyslaw W. Szymanski,[§] and Günter Allmaier*[,†]

[†]Institute of Chemical Technologies and Analytics, TU Wien, Getreidemarkt 9/164, A-1060 Vienna, Austria

[‡]Bijvoet Centre for Biomolecular Research and Utrecht Institute of Pharmaceutical Sciences, Utrecht University, NL-3584 CH Utrecht, The Netherlands

[§]Faculty of Physics, University of Vienna, A-1090 Vienna, Austria

[∥]Department of Medical Biochemistry, Max F. Perutz Laboratories, Medical University of Vienna, Vienna Biocenter (VBC), A-1030 Vienna, Austria

Supporting Information

ABSTRACT: Gas-phase electrophoretic mobility molecular analysis (GEMMA) separates nanometer-sized, single-charged particles according to their electrophoretic mobility (EM) diameter after transition to the gas-phase via a nano electrospray process. Electrospraying as a soft desorption/ionization technique preserves noncovalent biospecific interactions. GEMMA is therefore well suited for the analysis of intact viruses and subviral particles targeting questions related to particle size, bioaffinity, and purity of preparations. By correlating the EM diameter to the molecular mass (M_r) of standards, the M_r of analytes can be determined. Here, we demonstrate (i) the use of GEMMA in purity assessment of a preparation of a common cold virus (human rhinovirus serotype 2, HRV-A2) and (ii) the analysis of subviral HRV-A2 particles derived from such a preparation. (iii) Likewise, native mass spectrometry was employed to obtain spectra of intact HRV-A2 virions and empty viral capsids (B-particles). Charge state resolution for the latter allowed its M_r determination. (iv) Cumulatively, the data measured and published earlier were used to establish a correlation between the M_r and EM diameter for a range of globular proteins and the intact virions. Although a good correlation resulted from this analysis, we noticed a discrepancy especially for the empty and subviral particles. This demonstrates the influence of genome encapsulation (preventing analytes from shrinking upon transition into the gas-phase) on the measured analyte EM diameter. To conclude, GEMMA is useful for the determination of the M_r of intact viruses but needs to be employed with caution when subviral particles or even empty viral capsids are targeted. The latter could be analyzed by native MS.

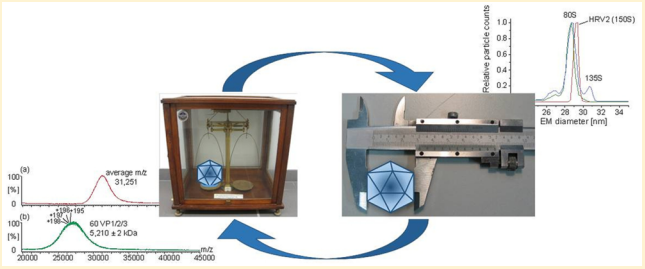

Gas-phase electrophoretic mobility molecular analysis (GEMMA) is applicable for the analysis of material in the single-digit nanometer size range up to particles of several hundred nanometers in diameter.[1−3] Lately, also other acronyms for the same type of instrument, such as macro Ion Mobility Spectrometer (macroIMS),[4,5] LiquiScan-ES (official instrument name for a short time given by the manufacturing company, TSI Inc.), ES-DMA,[6] or ES-SMPS spectrometer[7] appear in the literature. However, to remain consistent with work from our and other laboratories, the term "GEMMA" will be used throughout the manuscript.

GEMMA measurements are based on the separation of single-charged particles obtained from a nano electrospray (ES) source followed by charge reduction in a bipolar atmosphere using a ^{210}Po α-particle source. Particle separation is achieved by application of a laminar flow and an orthogonal electric field in a differential mobility analyzer (DMA)[1,2] that sorts analytes according to their respective electrophoretic mobility (EM) diameters. Particles of a given size (i.e., the EM diameter) pass through the mobility analyzer according to the applied electric field, **E**, in the DMA unit. Variation of **E**, at constant laminar flow, allows scanning of a given size range. Depending on the geometry of the DMA, particles within different size ranges can be measured.[8,9] These particles then act as condensation nuclei in a supersaturated atmosphere of either *n*-butanol or water in a condensation particle counter (CPC)[10] and are counted via passing through a focused laser beam. Analyte detection in the

Received: April 17, 2015
Accepted: July 25, 2015
Published: July 29, 2015

DOI: 10.1021/acs.analchem.5b01450
Anal. Chem. 2015, 87, 8709−8717

CPC is therefore exclusively based on the number of particles practically irrespective of their molecular mass (M_r) or chemical nature. Recent developments of GEMMA instruments (DMAs with laminar flow values of 50 L per minute (Lpm)[11] and even higher[12]) allow collection of spectra with excellent resolution (see Figure S1 for comparison of GEMMA spectra obtained with various GEMMA device generations using comparable samples).

Given that M_r standards of the same chemical nature as the analyte are available, the M_r of an analyte can be determined from its EM diameter.[1] This approach was first demonstrated with good statistics by Bacher and colleagues[3] for proteins up to approximately 2 MDa. However, extrapolation of this standard curve to human rhinovirus serotype 2 (HRV-A2) particles yielded a M_r deviating by as much as 36% from the value calculated from the sum of its building blocks (8085 kDa). This deviation was attributed to the lack of standards with higher M_r (considering that protein standards mostly well below 0.5 MDa were employed by Bacher et al.). Nevertheless, it could be demonstrated that GEMMA allows for measurements of M_r's by far exceeding the range currently accessible to standard mass spectrometry. Kaddis and colleagues[13] extended the original correlation curve to approximately 12 MDa by including cowpea chlorotic mottle virus (CCMV) and several forms of protein vaults, i.e., large ribonucleoprotein particles of ellipsoid shape found in eukaryotes. However, the M_r values of these particles were again calculated and not experimentally assessed, and as for HRV-A2, the EM diameter/M_r data point for CCMV deviated significantly from the fitted correlation curve. By the same token, the data points for vaults scattered substantially possibly because of the nonspherical nature of these latter analytes (see, e.g. ref 14). Despite these apparent challenges, GEMMA analyses are receiving increased attention in the field of virology as can be learned from the rapidly growing number of publications[15−23] including ours on HRV.[3,11,24−27]

HRV-A2 (a HRV genus A serotype 2) is a nonenveloped icosahedral virus of approximately 30 nm diameter as based on X-ray crystallography,[28] cryo-electron microscopy 3D image reconstruction (cryo-EM 3DR),[29] and previous GEMMA[3] measurements. It is composed of four viral proteins (VP1−4), 60 copies each, and a single stranded, positive sense RNA genome of approximately 7.1 kb length, covalently linked to a single copy of the peptide VPg.[30,31] During virus uncoating (i.e., the process of viral RNA transfer from the capsid into the cytosol of an infected cell), the protein shell undergoes conformational changes resulting in subviral particles; the intermediate A-particle has lost VP4 but still contains the RNA genome. On release of the RNA (together with VPg), the empty capsid, the B-particle, remains.[32] X-ray and cryo-EM 3DR reported an expansion of the subviral A and B particles by approximately 4% with respect to the native virus.[33,34]

Previous GEMMA analyses revealed an additional component in virus preparations (the "contaminant" first detected by capillary electrophoresis, CE[35]) of an EM diameter comparable to that of virions but of significantly higher heterogeneity.[27] We tentatively identified it as cellular membrane fragments. It is of note that only advancements in GEMMA instrumentation of the past decade allowed for the differentiation of intact HRV-A2 and the contaminant because previous setups only yielded one broad peak at the EM diameter of intact virus including both species (see Figure S1 for comparison of GEMMA spectra generated by various GEMMA device generations and comparable HRV-A2 samples).

Bacher et al.[3] demonstrated the conformational changes during virus uncoating via a GEMMA prototype instrument is possible and confirmed an approximately 4% increase in EM diameter on formation of empty capsids (B-particles). Here, we report now a repeat of these measurements with a more advanced GEMMA instrument.[11] A highly pure virus stock, a prerequisite for MS, electron microscopy, and GEMMA analyses,[36] was used to eliminate any possible impact of the contaminant on the measurements. Additionally, we intended to assess the M_r of viral and subviral particles via native MS, a technique based on volatilization of analytes via an ES ionization (ESI) process; their separation is occurring *in vacuo*. Moreover, no charge reduction takes place, instead analytes carry multiple charges. Despite these harsher conditions, the structure of large, noncovalent protein complexes (including viruses) is preserved during the complete analysis.[22,37−40] Finally, it was our intention to extend the M_r/EM diameter correlation previously described for proteins to the MDa range allowing M_r determination of globular viruses. Data for spherical virions, as compiled by Pease,[21] were included, as indicated in the respective figures, provided that their M_r values were accessible from experiments and not calculated by adding the M_r's of their components. The correlation established here between EM diameter and M_r for intact, spherical, native viruses now allows one to determine, via GEMMA, the M_r of viruses in general with greater precision than has been possible to date.

MATERIALS AND METHODS

Analyte and Reagents. HRV-A2 was prepared either according to standard protocols[41] (two preparations) or, in the case of highly pure virus preparations, according to a slightly changed protocol including a lipase (porcine pancreas, Sigma-Aldrich) digestion step (two preparations). In short, HRV-A2 was grown in a HeLa-H1 cell suspension culture. Repeated freezing/thawing cycles and pelleting of cell debris allowed recovery of virions from the supernatant. Subsequent purification steps included (i) pelleting of virions and (ii) enzymatic removal of contaminating protein, DNA, and RNA. The highly pure HRV-A2 preparations were obtained by including a digestion step with 0.2 U/μL lipase at 28 °C overnight by gently shaking on an Eppendorf thermomixer prior to step (ii). Finally, (iii), virions were pelleted and submitted to sucrose density gradient centrifugation. HRV-A2 containing fractions were recovered; the virus was pelleted via high-speed centrifugation, and the pellet was resuspended in 50 mM sodium borate (pH 7.4). For a detailed list of further chemicals as well as proteins employed for setup of a M_r/EM diameter correlation, refer to the Supporting Information.

Buffers and Solutions. CE background electrolyte (BGE) was 100 mM boric acid adjusted to pH 8.3 via sodium hydroxide and included 10 mM SDS. Ammonium acetate (NH_4OAc) at the indicated concentrations and pH values was employed as electrolyte for GEMMA and native ESI MS measurements. BGE and NH_4OAc was filtered through surfactant free cellulose acetate membrane, 0.20 μm pore size syringe filters (Sartorius, Göttingen, Germany). 0.1% TFA was obtained via mixing of a respective volume with water of Millipore grade. Sinapic acid as MALDI MS matrix was dissolved at 10 mg/mL in ACN/0.1% TFA (1:1; v/v).

DOI: 10.1021/acs.analchem.5b01450
Anal. Chem. 2015, 87, 8709−8717

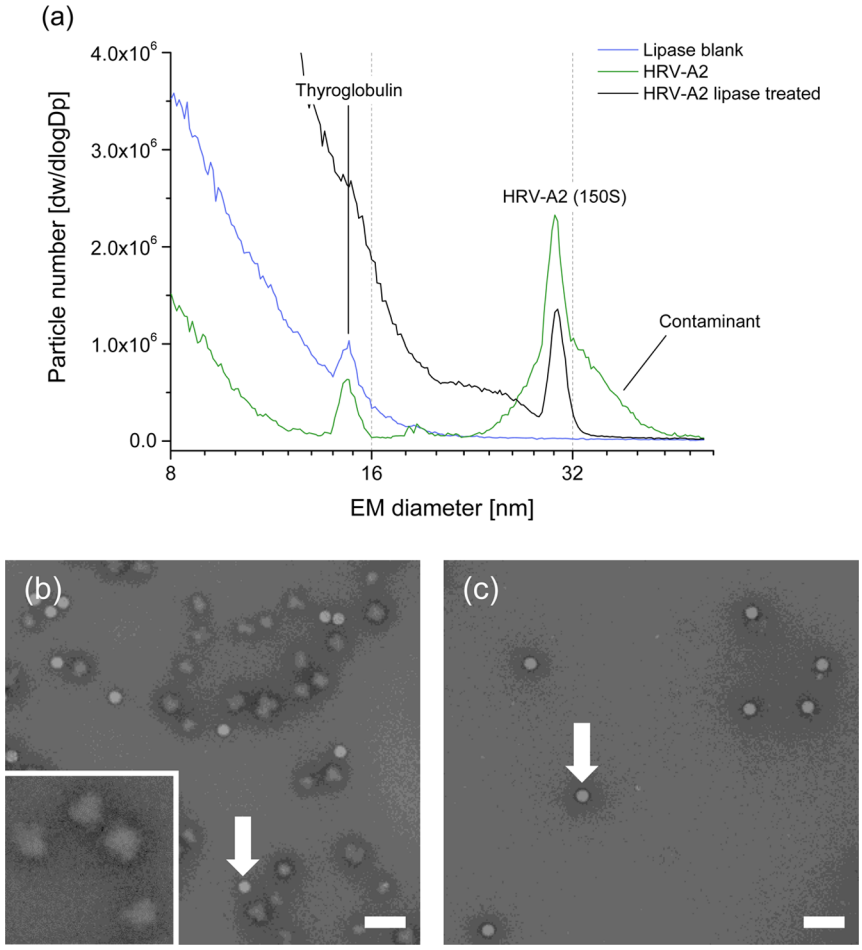

Figure 1. GEMMA spectra demonstrate that the contaminant of HRV-A2 preparations is sensitive to lipase digestion (a). Thyroglobulin is added as internal standard to allow easy comparison of spectra. TEM analysis of samples prior (b) and after digestion (c) with lipase; cloud-shaped contaminant (Cont.) material (enlarged in inset of (b)) disappears upon enzymatic treatment. Intact virions (marked by white arrows in TEM images) are not affected by digestion (100 nm size bar).

Instrumentation. CE and TEM measurements were carried out as described elsewhere in detail.[41] An additional overview is given in the supplement.

MALDI MS measurements of keyhole limpet hemocyanin (KLH) derivates were carried out by means of an Axima CFR$^+$ instrument (Shimadzu Kratos Analytical, Manchester, UK) in the linear, positive ion mode employing a Coval-X high mass detector (Zürich, Switzerland) and Fleximass DS MALDI MS targets (Shimadzu). For calibration, bovine γ-globulin (≥99%, Sigma-Aldrich, 10 pmol/μL in aqueous 0.1% TFA) was mixed with matrix solution and applied to the MALDI MS target.

In native mass spectrometry experiments, (tandem) mass spectra were recorded on a modified (MSVision, Almere, The Netherlands) Q-RTOF (Waters, Manchester, UK) instrument in positive ion mode[42] (native mass spectrometry analysis). Xenon was used as the collision gas to increase the transmission of viral particles.[43] Voltages and the pressure of the other gases were optimized for transmitting large noncovalent protein complexes.[44,45] For determination of the M_r of the empty capsids (B-particles), charges were assigned to the distribution that resulted in a derived M_r with the smallest standard deviation. Charge state assignment was further confirmed by theoretical simulation of the charge state distribution corresponding to the empty capsid (in absence of both VP4 and RNA) using the software SOMMS.[46]

Desalting of HRV-A2 Stock Solutions and Sample Preparation. Desalting and exchange of HRV-A2 stock storage buffer for NH_4OAc was carried out as described by using 10 kDa M_r cutoff spin filters (poly(ether sulfone) membrane from VWR, Vienna, Austria).[27] The HRV-A2 concentration of the desalted stock was calculated on the basis of (i) the initial virus concentration determined by CE,[41] (ii) sample dilution during desalting, and (iii) neglecting virus interaction with the membrane (which reduced the amount of a similar analyte by only roughly 20%). Hence, for simplification, a total recovery of the analyte from the filter was assumed. The two conventional HRV-A2 preparations used in this report were diluted in 50 mM NH_4OAc (pH 8.4) resulting in final virus stocks of 16 and 45 nM particle concentration, respectively. One of the two highly pure HRV-A2 preparations was diluted in 50 mM NH_4OAc (pH 8.4) and the other one in 10 mM NH_4OAc (pH 9.5), yielding final virus concentrations of 3 and 16 nM, respectively. We did not observe any influence of NH_4OAc concentrations and pH values on virus stability or recovery during desalting. Further details concerning the preparation of samples is given in the Supporting Information.

RESULTS AND DISCUSSION

It was one of the aims of the current study to (i) prepare HRV-A2 of high purity, (ii) to check its behavior in comparison to

DOI: 10.1021/acs.analchem.5b01450
Anal. Chem. 2015, 87, 8709−8717

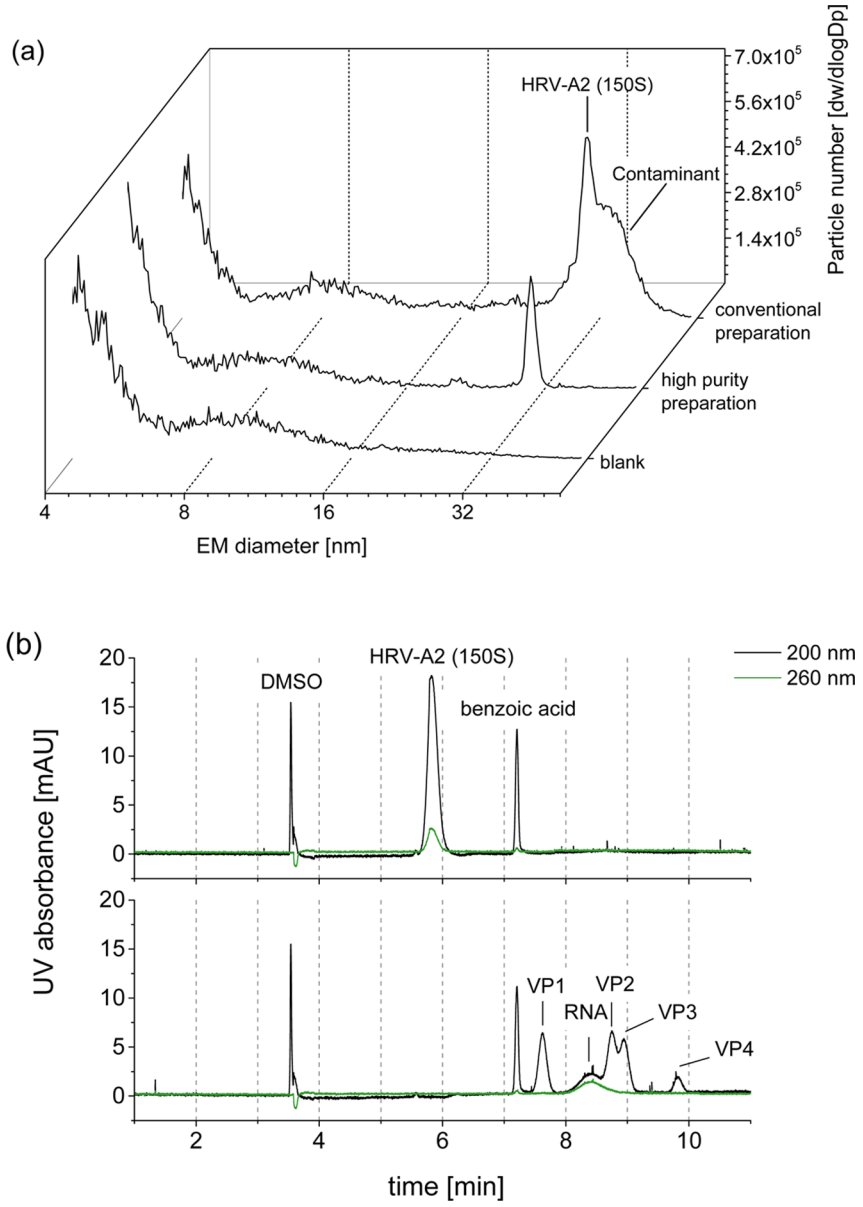

Figure 2. GEMMA and CE analyses of HRV-A2 preparations. (a) GEMMA spectra demonstrate that lipase digestion results in virus of high purity (components and products of the enzymatic digest are removed during the virus preparation process itself in contrast to Figure 1). (b) CE does not distinguish a conventional virus preparation (see ref 41) from a preparation involving lipase digestion (an exemplary electropherogram of the latter is shown).

virus preparations obtained via our conventional conditions, and (iii) to employ this highly pure HRV-A2 for GEMMA and native MS measurements, both based on an electrospray process, for the establishment of a M_r/EM diameter calibration curve applicable for virus M_r determination.

Preparation of Highly Pure HRV-A2 and Its Analysis via GEMMA. The contaminant present in conventional HRV-A2 preparations gave rise to a broad, heterogeneous peak in the GEMMA spectra; this and other unpublished data led us to assume that it was composed of lipid membrane fragments originating from host cells.[27] Indeed, GEMMA revealed that the corresponding peak was greatly diminished upon lipase digestion (Figure 1a), whereas the HRV-A2 peak was unchanged. Concomitant with the disappearance of the contaminating high M_r material, low M_r material with up to 16 nm EM diameter increased and most probably represents digested membrane fragments, enzyme aggregates, and/or buffer components of the added enzyme. TEM imaging underscores the GEMMA results and upon lipase digestion, the amount of irregularly shaped material (i.e., the contaminant) seen in the original sample (Figure 1b, enlarged in inset) was significantly reduced (Figure 1c). HRV-A2 particles (bright spheres indicated by arrows) were unaffected by the enzyme treatment.

The EM diameter distribution of the contaminant, as seen in GEMMA, varied strongly between HRV-A2 batches giving rise to different broad peaks.[27] We were not interested in the chemical nature of this component but rather concentrated on how to obtain HRV-A2 of the highest possible purity.

To remove the contaminant, we modified the conventional virus preparation protocol;[41] an additional lipase digestion step was included prior to the sucrose density gradient ultra-

DOI: 10.1021/acs.analchem.5b01450
Anal. Chem. 2015, 87, 8709−8717

centrifugation (see Materials and Methods section). As demonstrated in the GEMMA measurements depicted in Figure 2a, the modified protocol yielded virus of exceptional purity; no contaminating material was detectable.

We then compared two highly pure HRV-A2 preparations with batches obtained via the previously used standard purification protocol. (i) The virus concentrations of two highly pure preparations (1.1 ± 0.1 and 3.9 ± 0.6 mg/mL virions, n = 3, respectively) as determined via CE[41] (exemplary electropherogram in Figure 2b, top) were comparable to that of conventional preparations.[41] (ii) Upon incubation for 10 min at 56 °C in BGE,[47] CE resolved the four VPs and the viral RNA genome (exemplary electropherogram in Figure 2b, bottom); the CE profiles of all four batches were again indistinguishable. (iii) The specific infectivity ($TCID_{50}$/mL; 2.31×10^{11} and 4.14×10^{11}, respectively) was essentially the same for all four batches. From the number of intact virions (calculated from CE) and the number of infective particles ($TCID_{50}$/mL), the ratio of infective virions and the number of particles were calculated and were again very similar for batches prepared by either protocol. From these data, we conclude that the additional lipase incubation had no significant influence on virus yield and infectivity; only the contaminant was removed.

GEMMA Analysis of HRV-A2 Subviral Particles. Incubation of HRV-A2 at 56 °C or at acidic pH leads to formation of subviral A-particles and empty virions (B-particles) and, in the presence of SDS, to dissociation into individual components, the viral capsid proteins and the genomic RNA.[27,41,48] The (nonphysiologic) heating is believed to lead to unordered exit of the RNA genome instead of the well-coordinated release observed under close-to *in vivo* conditions.[34] Nevertheless, empty capsids were electrophoretically indistinguishable regardless of whether they were prepared via heating or exposure to acidic pH, as in the endosomal compartment during infection of host cells.[27] Therefore, to minimize matrix effects, we prepared empty capsids via heating of the purified virus.

A-particles, as well as empty capsids (B-particles), are expanded by about 4% in comparison to native virions.[33,34] Employing a commercial GEMMA as well as a custom-built instrument, we were able to measure the corresponding particles. However, due to the higher peak resolution, i.e., the full width at half maximum (fwhm) of the peak recorded for native virions was reduced by a factor of 3, which is brought about by a higher laminar sheath flow in the DMA unit;[11] we only present spectra obtained with the custom-built instrument (Figure 3). On incubation of HRV-A2 at 56 °C for 10 min, the original virus peak (containing particles as visualized by TEM) disappeared. Concomitantly, a new peak appeared. However, instead of the expected 4% increase in diameter, the position of the new peak rather corresponds to about a 2% decrease of the EM diameter (from 29.3 to 28.7 nm). Examination of the heated virus with negative stain TEM (Figure 3, inset) clearly identified it as (empty) B-particles. Interestingly, another subviral particle was found to possess a 5% larger EM diameter (30.6 nm); it likely corresponds to the A-particle with the same composition as the B-particle except that it still contains the RNA genome. With incubation of HRV-A2 at 56 °C, the conversion into empty shells appears not to be complete and A-particles are present to a minor extent.

On the basis of X-ray crystallography and cryo-EM image reconstruction, A- and B-particles have the same diameter in contrast to GEMMA results as presented in the preceding

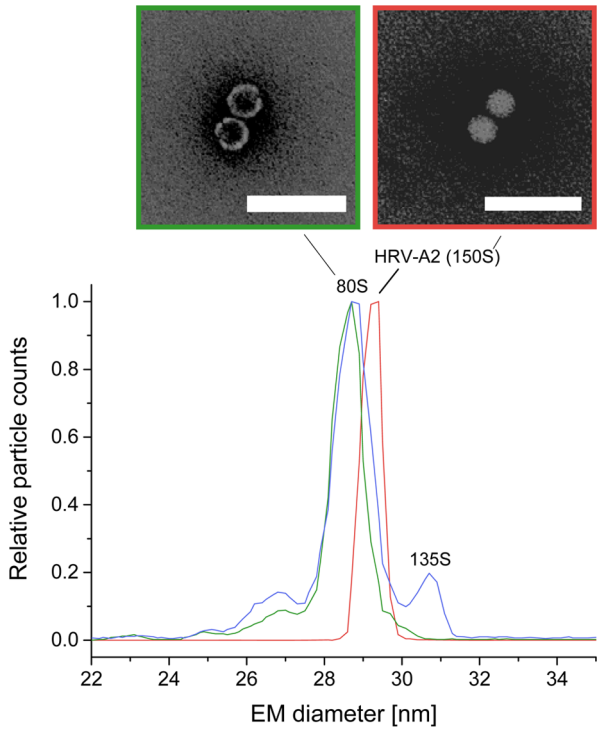

Figure 3. GEMMA analysis of viral and subviral particles on a custom-built instrument with high peak resolution allows for the separation of intact virions and subviral A- and empty B-particles. Spectra of three different samples containing mostly native virions (red), a substantial fraction of A-particles (blue), and mostly B-particles (green) are shown. The insets show TEM images of corresponding particles (100 nm size bar).

paragraph. Kaddis et al.[13] suggested that analytes in the course of GEMMA measurements are compressed upon transition to the gas-phase and hence exhibit a slightly lower EM diameter than in solution. These researchers also observed that components present within the protein assemblies (e.g., iron cores in ferritin) exert a stabilizing effect and thereby influence the observed EM diameters. Particles lacking these stabilizers appear smaller in GEMMA than their stabilized counterparts of the same M_r. The presence of RNA in A-particles, which exhibit a higher sedimentation constant (135S) in comparison to that of the empty B-particle (80S), might significantly decrease the shrinking of 135S particles upon transfer to the gas-phase (keep in mind that both subviral particles showed the same diameter in X-ray crystallography and cryo-EM). The well-documented expansion of the A-particle with respect to the native virus is clearly detected by GEMMA despite its lower M_r due to lack of VP4, corresponding to ~450 kDa in total (consider that the particle with lower M_r exhibits the larger EM diameter). The EM diameter increase of the A-particle, but not of the B-particle, is thus in good accordance with the data derived from X-ray crystallography and cryo electron microscopy.[33,34] The additional peaks with lower EM diameters (25.1 and 26.8 nm, respectively) might correspond to partially uncoated virions, broken capsids, or shells lacking a pentamer.

On the basis of the above results, we asked whether extrapolation of only one regression curve similar to the one presented by Bacher et al. for protein standards[3] might allow one to obtain M_r values from EM diameter data for various viral and subviral analytes (see final section of Results and Discussion).

DOI: 10.1021/acs.analchem.5b01450
Anal. Chem. 2015, 87, 8709−8717

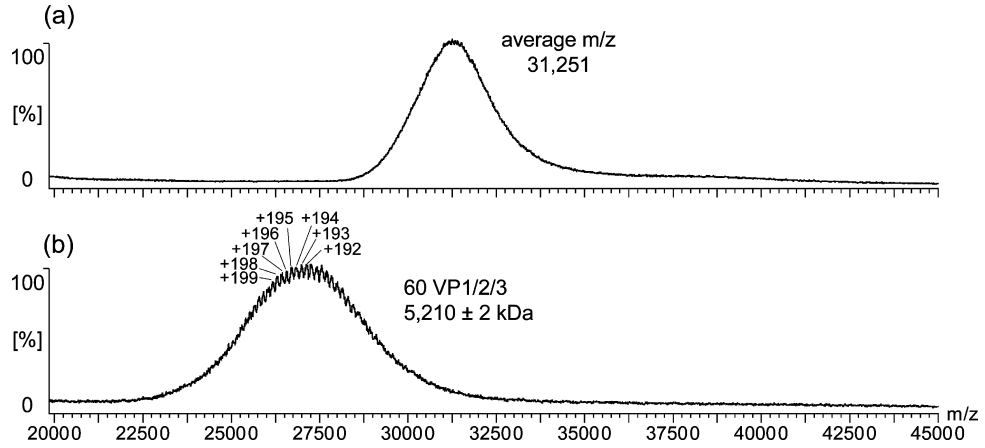

Figure 4. Positive ion mass spectra (native ESI MS) of (a) native HRV-A2 and (b) empty HRV-A2 capsids (B-particles). For the latter, charge state resolution can be obtained and a M_r calculated.

Native ESI MS. To correlate GEMMA-derived EM diameters with experimentally determined M_r's (instead of calculating them from the respective components), we attempted to determine the M_r of native viral 150S and subviral 80S particles by means of native MS (Figure 4). Fortunately, for both highly purified particles, we obtained Gaussian-shaped distributions of m/z values at very high m/z values. For the empty B-particles, charge state resolution of the distribution was obtained, a prerequisite for the M_r calculation from the experimental data. The charge state resolution could only be obtained from virus batches of high purity as produced with prior lipase digestion.

In contrast, native viral particles seem to be more heterogeneous; this heterogeneity might result from (i) differences in the length of the 3′ poly(A) tail of the viral genome or (ii) cations like polyamines that are taken up during virus assembly to neutralize excess charge of the anionic RNA. Therefore, an exact M_r determination via ESI MS was not possible; however, an average m/z value of 31 251 was obtained. Even incubation of virions for 4 h at 37 °C in NH_4OAc (conditions inducing viral breathing[49] to exchange encapsulated material for ammonium ions via diffusion) did not lead to increased charge state resolution. We thus assume that the differently sized poly(A) in intact virions are at the origin of these problems.

The M_r of (empty) B-particles was calculated to be 5210 ± 2 kDa from the native MS data. This is in perfect accordance with the theoretical value obtained by addition of the M_r values of 60 copies of each of the capsid proteins VP1 to VP3 (polyprotein P04936 from www.uniprot.org, vers. 157 from July 9, 2014, calculation via www.expasy.org) resulting in a value of 5209.5 kDa. To our knowledge, this is the first native MS-based M_r determination of intact HRV empty capsids.

We also investigated the stability of the empty capsids (Figure 5a) by probing their dissociation into VPs as a function of the collision energies employed in CID experiments (Figure 5b). Less stable particles are likely to dissociate at lower collision energies (and to a greater extent). Figure 5c demonstrates that VP1 readily dissociates from the empty viral shell suggesting that the VP1-interactions with its neighbors are weakened during virus uncoating. VP2 dissociates to a lesser extent, which could indicate that it is more strongly bound to its neighbors. In contrast, CID experiments performed on the native virion, instead, identified VP1 as undergoing the lowest level of dissociation (data not shown). It is thus likely that VP1 is more strongly bound to its symmetry-related copies than the other subunits of the virion, and the RNA genome. The latter is consistent with its reported interaction with the encapsulated nucleic acid.[34]

M_r/EM Diameter Correlation. We set up a protein-based EM diameter/M_r correlation ($corr_{new}$) as displayed in Figure 6 (see Figure S3 for experimental data). Data on other virus particles as described in the literature and compiled in ref 21 were included in $corr_{new}$ given that (i) they are spherical, (ii) the EM diameter values were reported from at least two individual sources, and (iii) M_r values had been accessed experimentally. Applying these criteria, data points for phage MS2[15,16,50−56] and rice yellow mottle virus (RYMV)[15,53,57] were included in $corr_{new}$ which had a value of $y = 0.03062x^{3.67155}$. For values below 15 nm EM diameter, this correlation and the composite curve described by Bacher et al.[3] are in very good accordance. However, since the newly recorded curve includes a higher number of proteins larger than 0.5 MDa, as well as two viruses, a steeper increase of $corr_{new}$ was obtained upon extrapolation to higher M_r values. Already for native HRV-A2 (29.9 ± 0.4 nm EM diameter), this resulted in differences of about 34% M_r. $Corr_{new}$ yielded M_r values much closer to the theoretical M_r of HRV-A2, ≥8085 kDa according to ref 3, than to the correlation previously reported (7982 kDa for $corr_{new}$ vs 5251 kDa as reported by Bacher et al.[3]). The theoretical M_r of intact HRV-A2 is about 1.3% higher than the value calculated via $corr_{new}$.

Data points for empty HRV-A2 (B-particles) as well as intermediate particles (135S) showed a considerable deviation from $corr_{new}$. This observation is of special importance for GEMMA measurements of viruses and subviral particles as considerations about the particle size and structure, especially concerning the stabilizing effect of the nucleic acid on the viral capsids, will allow M_r determination via GEMMA with increased accuracy.

■ CONCLUDING REMARKS

Addition of a lipase digestion step to our conventional HRV preparation protocol allowed for removal of a troublesome contamination always present to various degrees in our previous virus preparations. The highly pure virus obtained thereby was used for gas-phase electrophoretic mobility molecular analysis on a commercial GEMMA as well as on a

DOI: 10.1021/acs.analchem.5b01450
Anal. Chem. 2015, 87, 8709−8717

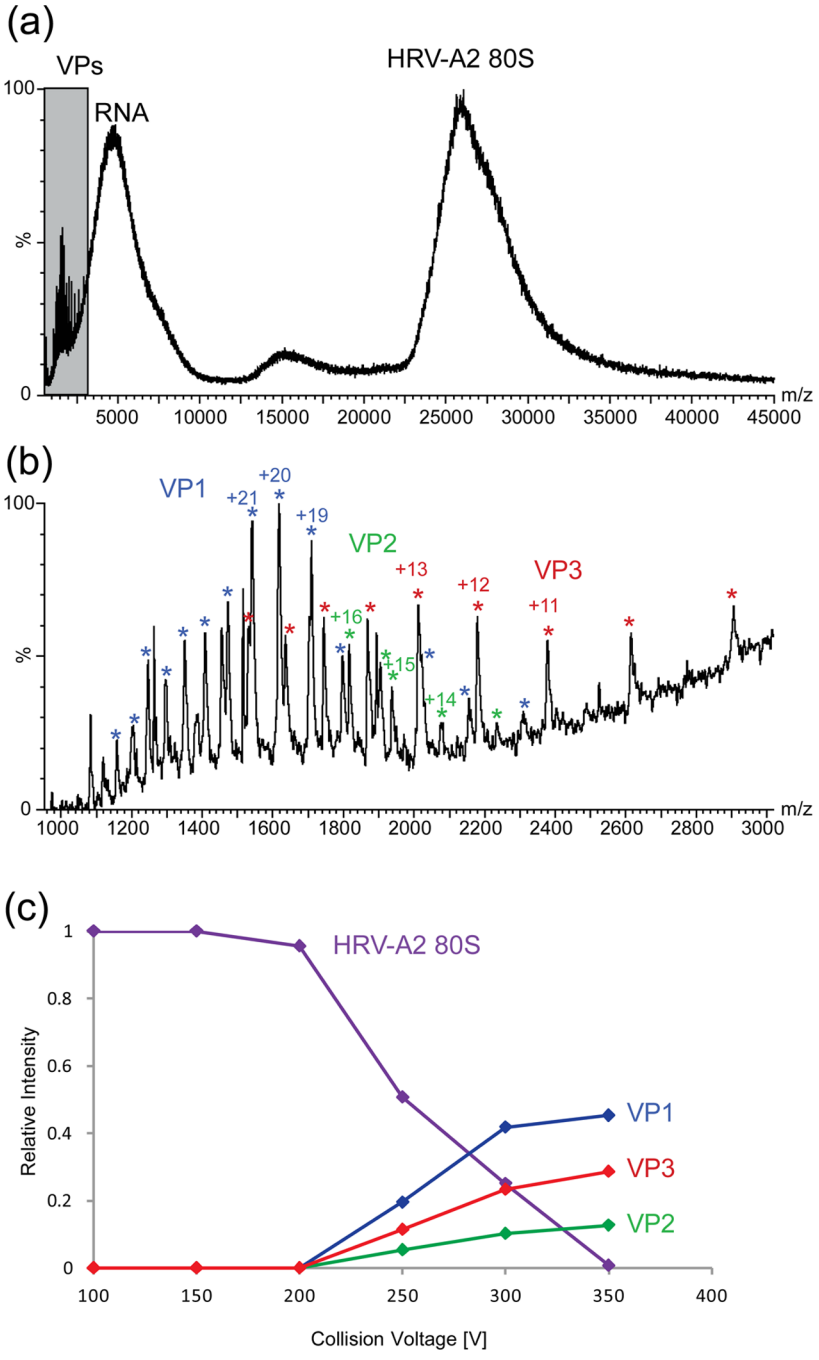

Figure 5. Positive ion CID analysis of empty HRV-A2 capsids (B-particles). At higher collision energies (example for 300 V is presented, (a)), the particles undergo gas-phase dissociation into the component VPs. Enlargement of the m/z region corresponding to the dissociated subunits (b) identifies VP1 (blue), VP2 (green), and VP3 (red). Ions in the respective distributions are indicated by "*" and in some cases with their charge states. The relative signal intensity of the free VPs with respect to that of empty capsids (violet) at different collision energies (c) provides information pertaining to the relative stability (i.e., binding strength) of the respective VP within the subviral assembly.

custom-built instrument (with higher nano DMA resolution) to analyze the native virus as well as its derived subviral particles. For the first time, we also successfully measured the same particles with native ESI MS. In the case of empty virions (B-particles), the resolution of charged states allowed for calculation of their M_r from the experimental data. The value fitted perfectly to the theoretically predicted M_r as calculated from the sum of the M_r's of its building blocks. Plotting M_r versus EM diameter of empty HRV-A2, we observed a clear deviation from the correlation curve ($corr_{new}$) obtained from proteins and two spherical viruses. It is of importance that (i) $corr_{new}$ already deviates from the M_r/EM diameter correlation based on proteins alone[3] and (ii) the theoretically predicted M_r of intact HRV-A2 virions fits exceptionally well to $corr_{new}$. Thus, $corr_{new}$ describes an improvement of correlations from the literature for native virus particles. The deviation of the theoretically predicted M_r value of HRV-A2 and the value calculated from its EM diameter via $corr_{new}$ lay within ±0.64% of an arithmetic mean.

DOI: 10.1021/acs.analchem.5b01450
Anal. Chem. 2015, 87, 8709−8717

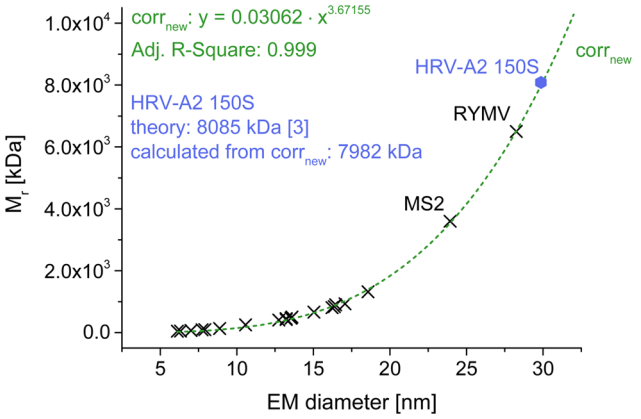

Figure 6. M_r/EM diameter correlation ($corr_{new}$) for proteins and two native virions (MS2 and RYMV). Inclusion of data points stemming from two viruses leads to a significant deviation of $corr_{new}$ from a protein-based correlation.[3] The M_r value for HRV-A2, as derived from its EM diameter using $corr_{new}$ (7982 kDa), deviates from the calculated sum of the M_r's of its building blocks (8085 kDa) by only ±0.64% of an arithmetic mean. Data points for empty HRV-A2 viral capsids are deviating significantly from the protein/virus particle-based correlation curve.

Regarding the expanded intermediates of HRV-A2 uncoating, we observed that the A-particle, that still contains the RNA but has a slightly reduced M_r because of loss of 60 copies of VP4, also exhibited a larger EM diameter than the intact virus. However, the empty B-particle, whose diameter is, based on X-ray and electron microscopy, identical to that of the A-particle had a much smaller EM diameter. It is thus obvious that various factors might influence the experimentally derived EM diameters of viruses and subviral particles. EM diameters are based on (i) the particle diameter *per se*, but (ii) the 3D-structure of the capsids (tight native virions vs porous uncoating intermediates) and (iii) encapsulated nucleic acid have to be taken into consideration as they might have profound effects on the transition of the particle into the gas-phase and its subsequent movement in the high laminar flow under the influence of a strong electric field.

The question, if protein standards can indeed be combined with viruses (a highly structured assembly of proteins and nucleic acids) to obtain a M_r/EM diameter correlation, cannot, at the moment, be answered finally. Neither proteins of sufficiently high M_r nor viruses of sufficiently low M_r are available for analysis in the necessary quality. Therefore, the combination of these two analyte classes appears reasonable for setting up a M_r/EM diameter correlation. Given that geometrical (spherical shape) as well as structural (native, compact virions composed of protein and RNA vs empty protein shells) constraints are regarded, GEMMA allows the M_r determination of analytes or bionanoparticles, which are not accessible via classical native MS approaches.

■ ASSOCIATED CONTENT

Supporting Information

The Supporting Information is available free of charge on the ACS Publications website at DOI: 10.1021/acs.analchem.5b01450.

Additional information on chemicals and reagents, instrumentation, and sample preparation; GEMMA spectra obtained with various GEMMA device generations using comparable samples; instrumental settings for GEMMA analyses; data employed for setup of a M_r/EM diameter correlation (PDF)

■ AUTHOR INFORMATION

Corresponding Author

*E-mail: guenter.allmaier@tuwien.ac.at. Tel: +43 1 58801 15160. Fax: +43 1 58801 16199.

Notes

The authors declare no competing financial interest.

■ ACKNOWLEDGMENTS

This work was supported by Austrian Science Foundation (FWF) Grants TRP29-N20 (to G.A. and W.W.S.), P25749-B20 (to V.U.W.), and P20915-B13 (to D.B.) as well as by ALW-ECHO 819.02.10 (to A.J.R.H.). This work was also supported by the Proteins@Work project, a program of The Netherlands Proteomics Centre financed by The Netherlands Organization for Scientific Research (NWO) as part of the National Roadmap Large-scale Research Facilities of The Netherlands (project number 184.032.201).

■ REFERENCES

(1) Kaufman, S. L.; Skogen, J. W.; Dorman, F. D.; Zarrin, F.; Lewis, K. C. *Anal. Chem.* **1996**, *68* (11), 1895−904.
(2) de la Mora, J. F.; de Juan, L.; Eichler, T.; Rosell, J. *TrAC, Trends Anal. Chem.* **1998**, *17* (6), 328−39.
(3) Bacher, G.; Szymanski, W. W.; Kaufman, S. L.; Zollner, P.; Blaas, D.; Allmaier, G. *J. Mass Spectrom.* **2001**, *36* (9), 1038−1052.
(4) Carazzone, C.; Raml, R.; Pergantis, S. A. *Anal. Chem.* **2008**, *80* (15), 5812−8.
(5) Kapellios, E. A.; Karamanou, S.; Sardis, M. F.; Aivaliotis, M.; Economou, A.; Pergantis, S. A. *Anal. Bioanal. Chem.* **2011**, *399* (7), 2421−33.
(6) Elzey, S.; Tsai, D. H.; Yu, L. L.; Winchester, M. R.; Kelley, M. E.; Hackley, V. A. *Anal. Bioanal. Chem.* **2013**, *405* (7), 2279−88.
(7) Shah, V. B.; Orf, G. S.; Reisch, S.; Harrington, L. B.; Prado, M.; Blankenship, R. E.; Biswas, P. *Anal. Bioanal. Chem.* **2012**, *404* (8), 2329−38.
(8) Flagan, R. C. *Aerosol Sci. Technol.* **1998**, *28* (4), 301−80.
(9) Intra, P.; Tippayawong, N. *J. Sci. Technol.* **2008**, *30* (2), 243−256.
(10) Koropchak, J. A.; Sadain, S.; Yang, X.; Magnusson, L. E.; Heybroek, M.; Anisimov, M.; Kaufman, S. L. *Anal. Chem.* **1999**, *71* (11), 386A−94A.
(11) Kallinger, P.; Weiss, V. U.; Lehner, A.; Allmaier, G.; Szymanski, W. W. *Particuology* **2013**, *11* (1), 14−9.
(12) Martinez-Lozano, P.; de la Mora, J. F. *J. Aerosol Sci.* **2006**, *37* (4), 500−12.
(13) Kaddis, C. S.; Lomeli, S. H.; Yin, S.; Berhane, B.; Apostol, M. I.; Kickhoefer, V. A.; Rome, L. H.; Loo, J. A. *J. Am. Soc. Mass Spectrom.* **2007**, *18* (7), 1206−16.
(14) Tanaka, H.; Tsukihara, T. *Proc. Jpn. Acad., Ser. B* **2012**, *88* (8), 416−33.
(15) Thomas, J. J.; Bothner, B.; Traina, J.; Benner, W. H.; Siuzdak, G. *Spectroscopy* **2004**, *18* (1), 31−6.
(16) Cole, K. D.; Pease, L. F., 3rd; Tsai, D. H.; Singh, T.; Lute, S.; Brorson, K. A.; Wang, L. *J. Chromatogr. A* **2009**, *1216* (30), 5715−22.
(17) Pease, L. F., 3rd; Lipin, D. I.; Tsai, D. H.; Zachariah, M. R.; Lua, L. H.; Tarlov, M. J.; Middelberg, A. P. *Biotechnol. Bioeng.* **2009**, *102* (3), 845−55.
(18) Guha, S.; Pease, L. F., 3rd; Brorson, K. A.; Tarlov, M. J.; Zachariah, M. R. *J. Virol. Methods* **2011**, *178* (1−2), 201−8.
(19) Pease, L. F., 3rd; Tsai, D. H.; Brorson, K. A.; Guha, S.; Zachariah, M. R.; Tarlov, M. J. *Anal. Chem.* **2011**, *83* (5), 1753−9.
(20) Guha, S.; Li, M.; Tarlov, M. J.; Zachariah, M. R. *Trends Biotechnol.* **2012**, *30* (5), 291−300.

DOI: 10.1021/acs.analchem.5b01450
Anal. Chem. 2015, 87, 8709−8717

(21) Pease, L. F., 3rd *Trends Biotechnol.* **2012**, *30* (4), 216−24.
(22) Bereszczak, J. Z.; Havlik, M.; Weiss, V. U.; Marchetti-Deschmann, M.; van Duijn, E.; Watts, N. R.; Wingfield, P. T.; Allmaier, G.; Steven, A. C.; Heck, A. J. *Anal. Bioanal. Chem.* **2014**, *406* (5), 1437−46.
(23) Havlik, M.; Marchetti-Deschmann, M.; Friedbacher, G.; Messner, P.; Winkler, W.; Perez-Burgos, L.; Tauer, C.; Allmaier, G. *Analyst* **2014**, *139* (6), 1412−9.
(24) Allmaier, G.; Laschober, C.; Szymanski, W. W. *J. Am. Soc. Mass Spectrom.* **2008**, *19* (8), 1062−8.
(25) Laschober, C.; Wruss, J.; Blaas, D.; Szymanski, W. W.; Allmaier, G. *Anal. Chem.* **2008**, *80* (6), 2261−4.
(26) Allmaier, G.; Maißer, A.; Laschober, C.; Messner, P.; Szymanski, W. W. *TrAC, Trends Anal. Chem.* **2011**, *30* (1), 123−32.
(27) Weiss, V. U.; Subirats, X.; Pickl-Herk, A.; Bilek, G.; Winkler, W.; Kumar, M.; Allmaier, G.; Blaas, D.; Kenndler, E. *Electrophoresis* **2012**, *33* (12), 1833−41.
(28) Verdaguer, N.; Blaas, D.; Fita, I. *J. Mol. Biol.* **2000**, *300* (5), 1179−94.
(29) Hewat, E. A.; Blaas, D. *EMBO J.* **1996**, *15* (7), 1515−1523.
(30) Fuchs, R.; Blaas, D. *Rev. Med. Virol.* **2010**, *20* (5), 281−97.
(31) Fuchs, R.; Blaas, D. *Adv. Virol.* **2012**, *2012*, 826301.
(32) Lonberg-Holm, K.; Yin, F. H. *J. Virol.* **1973**, *12* (1), 114−123.
(33) Garriga, D.; Pickl-Herk, A.; Luque, D.; Wruss, J.; Caston, J. R.; Blaas, D.; Verdaguer, N. *PLoS Pathog.* **2012**, *8* (1), e1002473.
(34) Pickl-Herk, A.; Luque, D.; Vives-Adrian, L.; Querol-Audi, J.; Garriga, D.; Trus, B. L.; Verdaguer, N.; Blaas, D.; Caston, J. R. *Proc. Natl. Acad. Sci. U. S. A.* **2013**, *110* (50), 20063−8.
(35) Kremser, L.; Petsch, M.; Blaas, D.; Kenndler, E. *Electrophoresis* **2006**, *27* (5−6), 1112−21.
(36) Weiss, V. U.; Kerul, L.; Kallinger, P.; Szymanski, W. W.; Marchetti-Deschmann, M.; Allmaier, G. *Anal. Chim. Acta* **2014**, *841* (100), 91−8.
(37) Uetrecht, C.; Versluis, C.; Watts, N. R.; Roos, W. H.; Wuite, G. J.; Wingfield, P. T.; Steven, A. C.; Heck, A. J. *Proc. Natl. Acad. Sci. U. S. A.* **2008**, *105* (27), 9216−20.
(38) Uetrecht, C.; Versluis, C.; Watts, N. R.; Wingfield, P. T.; Steven, A. C.; Heck, A. J. *Angew. Chem., Int. Ed.* **2008**, *47* (33), 6247−51.
(39) Shoemaker, G. K.; van Duijn, E.; Crawford, S. E.; Uetrecht, C.; Baclayon, M.; Roos, W. H.; Wuite, G. J.; Estes, M. K.; Prasad, B. V.; Heck, A. J. *Mol. Cell. Proteomics* **2010**, *9* (8), 1742−51.
(40) Snijder, J.; Rose, R. J.; Veesler, D.; Johnson, J. E.; Heck, A. J. *Angew. Chem., Int. Ed.* **2013**, *52* (14), 4020−3.
(41) Weiss, V. U.; Subirats, X.; Kumar, M.; Harutyunyan, S.; Goesler, I.; Kowalski, H.; Blaas, D. *Methods Mol. Biol.* **2015**, *1221*, 101−128.
(42) van den Heuvel, R. H.; van Duijn, E.; Mazon, H.; Synowsky, S. A.; Lorenzen, K.; Versluis, C.; Brouns, S. J.; Langridge, D.; van der Oost, J.; Hoyes, J.; Heck, A. J. *Anal. Chem.* **2006**, *78* (21), 7473−83.
(43) Lorenzen, K.; Versluis, C.; van Duijn, E.; van den Heuvel, R. H. H.; Heck, A. J. R. *Int. J. Mass Spectrom.* **2007**, *268* (2−3), 198−206.
(44) Tahallah, N.; Pinkse, M.; Maier, C. S.; Heck, A. J. *Rapid Commun. Mass Spectrom.* **2001**, *15* (8), 596−601.
(45) Sobott, F.; Hernandez, H.; McCammon, M. G.; Tito, M. A.; Robinson, C. V. *Anal. Chem.* **2002**, *74* (6), 1402−7.
(46) van Breukelen, B.; Barendregt, A.; Heck, A. J.; van den Heuvel, R. H. *Rapid Commun. Mass Spectrom.* **2006**, *20* (16), 2490−6.
(47) Kremser, L.; Bilek, G.; Kenndler, E. *Electrophoresis* **2007**, *28* (20), 3684−90.
(48) Subirats, X.; Weiss, V. U.; Gosler, I.; Puls, C.; Limbeck, A.; Allmaier, G.; Kenndler, E. *Electrophoresis* **2013**, *34* (11), 1600−9.
(49) Kremser, L.; Okun, V. M.; Nicodemou, A.; Blaas, D.; Kenndler, E. *Anal. Chem.* **2004**, *76* (4), 882−7.
(50) Eninger, R. M.; Hogan, C. J.; Biswas, P.; Adhikari, A.; Reponen, T.; Grinshpun, S. A. *Aerosol Sci. Technol.* **2009**, *43* (4), 298−304.
(51) Wick, C. H.; McCubbin, P. E. *Toxicol. Methods* **1999**, *9* (4), 245−252.
(52) Kuzmanovic, D. A.; Elashvili, I.; Wick, C.; O'Connell, C.; Krueger, S. *Structure* **2003**, *11* (11), 1339−1348.
(53) Wick, C. H.; Elashvili, I.; McCubbin, P. E.; Birenzvige, A. *Determination of MS2 Bacteriophage Stability at High Temperatures Using the Integrated Virus Detection System (IVDS)*; Report Number ECBC-TR-463; Edgewood Chemical Biological Center, U.S. Army: Aberdeen Proving Ground, MD, 2005.
(54) Hogan, C. J., Jr.; Kettleson, E. M.; Ramaswami, B.; Chen, D. R.; Biswas, P. *Anal. Chem.* **2006**, *78* (3), 844−52.
(55) Kuzmanovic, D. A.; Elashvili, I.; O'Connell, C.; Krueger, S. *Radiat. Phys. Chem.* **2008**, *77* (3), 215−24.
(56) Jung, J. H.; Lee, J. E.; Kim, S. S. *Anal. Chem.* **2009**, *81* (8), 2985−90.
(57) Fuerstenau, S. D.; Benner, W. H.; Thomas, J. J.; Brugidou, C.; Bothner, B.; Siuzdak, G. *Angew. Chem., Int. Ed.* **2001**, *40* (3), 541−544.

DOI: 10.1021/acs.analchem.5b01450
Anal. Chem. 2015, 87, 8709−8717